Liquid Crystals
Publication details, including instructions for authors and subscription information:
http://www.informaworld.com/smpp/title~content=t713926090

Modelling the molecular distribution in chevron FLCDs

Arnout de Meyere[a]; Ingolf Dahl[b]
[a] Department of Electronics and Information Systems, University of Gent, Sint-Pietersnieuwstraat 41, Gent, Belgium [b] Physics Department, Chalmers University of Technology, Göteborg, Sweden

To cite this Article de Meyere, Arnout and Dahl, Ingolf(1994) 'Modelling the molecular distribution in chevron FLCDs', Liquid Crystals, 17: 3, 397 — 412
To link to this Article: DOI: 10.1080/02678299408036579
URL: http://dx.doi.org/10.1080/02678299408036579

LIQUID CRYSTALS, 1994, VOL. 17, NO. 3, 397–412

Modelling the molecular distribution in chevron FLCDs

by ARNOUT DE MEYERE*
Department of Electronics and Information Systems,
University of Gent, Sint-Pietersnieuwstraat 41, B-9000 Gent, Belgium

and INGOLF DAHL
Physics Department, Chalmers University of Technology,
S-41296 Göteborg, Sweden

(*Received 10 September 1993; accepted 31 January 1994*)

Formulae are calculated for the main contributions to the energy in FLC-cells in the one-dimensional case. Special emphasis is given to the modelling of the smectic layers and to the influence of the electric field. For the study of structural questions in FLCDs, an efficient numeric simulation method is proposed. The use of it is illustrated with an example.

1. Introduction

In ferroelectric liquid crystal displays (FLCDs) the molecules are arranged in layers. At the moment when the display is filled, the liquid crystal material is isotropic, since it has been heated. On cooling down, it transforms into the nematic phase and later into the smectic A phase, where the layer structure appears. In order to have the molecules (which are perpendicular to the layers) parallel with the glass plates, the smectic layers must be planar and vertical. This is the so-called 'bookshelf'-structure. The inter-layer distance λ_A is approximately equal to the molecular length. At the final transition to the smectic C phase however, this inter-layer distance decreases and the molecules are tilted with respect to the layers. Since the smectic layers are pinned at the alignment coating on the glass plates, the only way to reduce their mutual distance is by tilting. The most probable geometry is shown in figure 1. It is called the chevron structure. There is an angle θ between the molecules and the layer normal. The molecules can rotate on a cone around this layer normal.

Since the invention of the surface stabilized FLCDs [1], the smectic C* layer structure has been a topic of intense research and discussion. After high resolution X-ray and optical response measurements, the first model with bookshelf geometry was modified to describe inclined and bent layers [2–4]. Important adjustments of the theory came with the introduction of the chevron structure [5–7].

A very important parameter is the layer tilt δ (see figure 1), since it has a great influence on the optical contrast of the final display. Are the layers composed of planar parts (as in figure 1) or is there a smooth curvature form one tilt angle to the other? Also the influence of an applied electric field on the position of the molecules and the bending of the layers is important for understanding the optical behaviour of the bistable device. Early arguments for a strong layer bending [8, 9] have been vitiated by X-ray

* Author for correspondence.

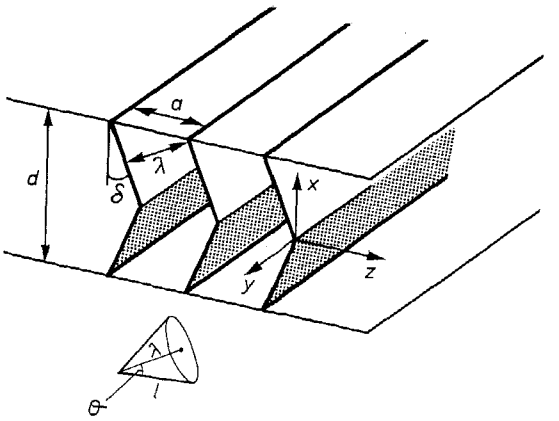

Figure 1. In the chevron structure, the smectic layers are tilted in a symmetrical way. The layer tilt angle is δ. The angle θ between the molecules and the layer normal is typical for the S_C phase. An important feature of the classical chevron structure is the $\delta - \theta$ coupling. A bending of the layer results in a change of the interlayer distance and hence of the smectic cone angle.

experiments [10–12]. Optical wave-guide measurements [13] confirm the idea of a very sharp chevron-tip.

An important help in the interpretation of the different results from measurement would be a usable continuum theory. For twenty years, researchers have been trying to form an optimal energetical description of smectic C* liquid crystals—see de Gennes [14], Dahl [15] and [16], and Nakagawa [17]. To a large extent the results agree. However, especially the compressibility of the layers is dealt with in different ways.

Due to the complexity of the expressions, computer programs are under development many years later than their nematic counterparts. Macgregor [18] has published a method for computing smectic layer structure based on Dahl's energy expressions. Recently, Leslie [19] presented theoretical considerations on flow effects in continuum theory for smectic liquid crystals, and his expressions are related to those published by Nakagawa.

In this paper, we describe a simplified version of the energy expressions, based on Dahl's equations. We consider planar FLC-cells with the smectic layer normal confined to one plane; orthogonal to the glass plates. In this case, the calculations are one dimensional. Closed analytical forms for the different contributions are presented. The simplifications allow for some straightforward interpretations and computer implementations. In this way, we are looking for theoretical foundations for the experimental data concerning the chevron profiles and molecular distribution in SSFLCDs.

2. Reference frames and vectors

Figure 2 shows the coordinate systems that we used. The *xyz* system is the usual reference frame with the x axis perpendicular to the glass plates, and the z axis parallel to the rubbing direction.

The *cpk* system is used for calculating elastic energies according to the expressions of Dahl [15, 16]. The k axis is the smectic cone axis. An arbitrary orientation of the cone requires two angles. We study the situation where **k** remains in the *xz* phase. In that

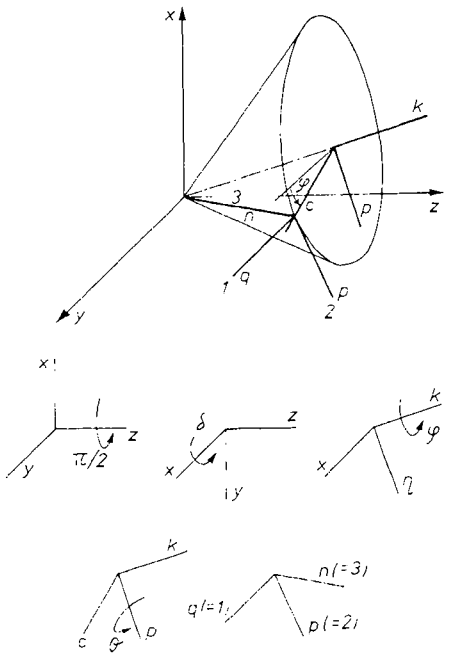

Figure 2. Five coordinate systems which transform into each other through a simple rotation about one of the coordinate axes. The *xyz* system is the usual lab reference frame. The *cpk* system and the molecular *qpn* axes are used for calculating elastic energies.

case the smectic layers are cylindrical and perpendicular to the *xz* plane. The orientation of **k** is then fully described with a tilt angle δ from the horizontal *yz* plane. Further rotation of *cpk* delivers the 123 or *qpn* axes connected with the liquid crystal molecule. The coordinates of **n** could be used if one prefers to describe the elastic forces with the nematic Oseen–Frank expressions.

By means of consequent rotations, one can derive the coordinates of the important vectors in a straightforward way. In order to result in the right order of the molecular axes, a preliminary rotation (+ 90 degrees around the *z* axis) of the lab frame *xyz* has been executed. The rotated vectors can be expressed as a linear combination of the (**x**, **y**, **z**) vectors in the following way

$$\left.\begin{aligned} (\mathbf{c}\quad \mathbf{p}\quad \mathbf{k}) &= (\mathbf{x}\quad \mathbf{y}\quad \mathbf{z})\cdot \mathscr{S} \\ (\mathbf{q}\quad \mathbf{p}\quad \mathbf{n}) &= (\mathbf{x}\quad \mathbf{y}\quad \mathbf{z})\cdot \mathscr{T}, \end{aligned}\right\} \quad (1$$

$$\mathscr{S} = \begin{pmatrix} -\sin\varphi\cos\delta & -\cos\varphi\cos\delta & \sin\delta \\ \cos\varphi & -\sin\varphi & 0 \\ \sin\varphi\sin\delta & \cos\varphi\sin\delta & \cos\delta \end{pmatrix},$$

$$\mathscr{T} = \begin{pmatrix} -\cos\theta\sin\varphi\cos\delta - \sin\theta\sin\delta & -\cos\varphi\cos\delta & -\sin\theta\sin\varphi\cos\delta + \cos\theta\sin\delta \\ \cos\theta\cos\varphi & -\sin\varphi & \sin\theta\cos\varphi \\ \cos\theta\sin\varphi\sin\delta - \sin\theta\cos\delta & \cos\varphi\sin\delta & \sin\theta\sin\varphi\sin\delta + \cos\theta\cos\delta \end{pmatrix}.$$

The columns of the transformation matrices $\mathscr{S}$ and $\mathscr{T}$ contain the coordinates of the transformated vectors in the xyz system. As a short notation we can therefore write

$$\mathscr{S} = \begin{pmatrix} c_1 & p_1 & k_1 \\ c_2 & p_2 & k_2 \\ c_3 & p_3 & k_3 \end{pmatrix},$$

$$\mathscr{T} = \begin{pmatrix} q_1 & p_1 & n_1 \\ q_2 & p_2 & n_2 \\ q_3 & p_3 & n_3 \end{pmatrix}.$$

Using this notation, other quantities, such as the matrix representation of the ε-tensor can be determined. In the fully rotated qpn system, the permittivity tensor is as follows:

$$\bar{\varepsilon}' = \begin{pmatrix} \varepsilon_1 & 0 & 0 \\ 0 & \varepsilon_2 & 0 \\ 0 & 0 & \varepsilon_3 \end{pmatrix},$$

(in the general biaxial treatment). The representation in the xyz system is obtained with the following transformation law

$$\bar{\varepsilon} = \mathscr{T} \bar{\varepsilon}' \mathscr{T}^{-1}.$$

$\mathscr{T}$ can be obtained with equation (1). Since **q**, **p** and **n** are orthogonal unit vectors, $\mathscr{T}^{-1}$ is just given by $\mathscr{T}^t$, the transpose of $\mathscr{T}$.

For the most frequent component one obtains

$$\begin{aligned} \varepsilon_{xx} &= \varepsilon_1 + p_1^2(\varepsilon_2 - \varepsilon_1) + n_1^2(\varepsilon_3 - \varepsilon_1) \\ &= \varepsilon_1 + p_1^2 \partial\varepsilon + n_1^2 \Delta\varepsilon. \end{aligned} \tag{2}$$

With the usual uniaxial approximation, $\varepsilon_1 = \varepsilon_2 = \varepsilon_\perp$ and $\varepsilon_3 = \varepsilon_\parallel$, equation (2) changes into

$$\begin{aligned} \varepsilon_{xx} &= \varepsilon_\perp + n_1^2 \Delta\varepsilon \\ &= \varepsilon_\perp + (-\sin\theta \sin\varphi \cos\delta + \cos\theta \sin\delta)^2 \Delta\varepsilon. \end{aligned} \tag{3}$$

Those expressions are similar to those mentioned in the literature—see [20] and [21].

3. Energies

The energy stored in the liquid crystal system can be divided into a volume term and a surface contribution

$$\mathscr{F} = \int_V f_{\text{vol}} dv + \int_S f_{\text{surf}} ds. \tag{4}$$

In its turn, the volume energy density has two main contributions: the elastic and the electric energy

$$f_{\text{vol}} = f_{\text{elas}} + f_{\text{elec}}.$$

All these energy contributions contain derivatives of the vectors considered above. Instead of making derivatives of the complicated coordinates, it is better to consider the transformation of each vector into linear combinations of the basic systems. Just as an example

$$\frac{\partial \mathbf{k}}{\partial \delta} = -\sin\varphi\,\mathbf{c} - \cos\varphi\,\mathbf{p}.$$

Let us discuss the different energy contributions one by one.

3.1. *Elastic energy*

3.1.1. *Incorporation of the layer structure*

The layer structure is often handled by introducing a vector along the layer normal (**k**), the length of which is a measure of the layer separation (see for example Dahl [16] or Nakagawa [22]). The crucial point is to come up with a decent formulation for the energy cost of layer thickness variations. Let us use the notation f_λ for this contribution.

3.1.1.1. *Layer thickness and cone angle*

Variations of the layer thickness are connected with changes of the cone angle θ. The situation is clarified in figure 1.

The following relations are easily verified:

$$\begin{aligned} \lambda &= l\cos\theta, \\ &= a\cos\delta, \\ \cos\theta &= \nu\cos\delta, \end{aligned} \tag{5}$$

with

$$\nu = \frac{a}{l},$$

where l is the molecular length and a the distance between the layers along the z axis, the rubbing direction. This parameter a is in fact defined by the way in which the transition from smectic A to smectic C occurred. If the layers stick perfectly to the alignment layers during the transition, then a equals λ_A, the layer distance in the smectic A phase. Notice that the number of molecules between two layers is determined by this parameter, since it defines the volume between the layers.

Equation (5) indicates a coupling between δ and θ. Especially in the one-dimensional approach that we are dealing with, a (and therefore ν) has to be constant. Hence, in this case, each variation of δ causes variations of θ, which are very hard to establish.

At this point, we want to refer to an important recent article by Willis *et al.* [10]. X-ray measurements show that the compressed region, at the tip of the chevron, is only a small fraction of the total display thickness. This observation agrees with the coupling between δ and θ. The elastic constant which expresses the energy of layer compression will be chosen to be sufficiently large, so that simulations confirm the thin compressed region. All of our considerations are within the frame of defect-free chevron structures. We agree that layering defects as suggested in [10] need a more complicated approach.

3.1.1.2. *Expressions for the layer compression energy*

Willis *et al.* [10], use the following expression for the layer compression energy

$$f_\lambda^* = T\left(\frac{\lambda - \lambda_0}{\lambda_0}\right)^2 = T\left(\frac{\cos\delta - \cos\delta_0}{\cos\delta_0}\right)^2, \tag{6}$$

where λ is the actual layer thickness, while λ_0 is the undeformed layer thickness, without compression or dilation; δ and δ_0 are the corresponding layer tilt angles.

Another, very similar equation has been formulated in [16]. An expression is given for the 'distension' (negative of compression) of the layers

$$\gamma \equiv 1 - \frac{\lambda_0}{\lambda}.$$

The energy contribution due to the layer thickness variations can be written as follows—see [16].

$$f_\lambda^\bullet = T\gamma^2.$$

Still another possibility could be

$$f_\lambda^\dagger = T(\lambda^2 - \lambda_0^2)^2$$

which is similar to the one mentioned in [23].

If one wants to stress the relationship with the smectic cone angle,

$$f_\lambda^\circ = T\sin^2(\theta - \theta_0)$$

could be used, as has been done in [24].

3.1.2. *Expressions for the elastic energy*

3.1.2.1. *Oseen–Frank*

Early papers on ferroelectric liquid crystals still used some modified form of the nematic Oseen–Frank expression for the elastic energy. Nowadays, most authors use the more sophisticated description mentioned in the introduction. Nevertheless, it can be useful to compare the main contributions to the elastic energy in the classical and modern approach.

In the case that angles only vary along the x-direction (1-dimensional approach), the Oseen–Frank expression with equal elastic constants ($K_1 = K_2 = K_3 = K$) and $q_\parallel = q_\perp = 0$ is as follows:

$$\begin{aligned} f_{OF} &= \tfrac{1}{2}K((\nabla\cdot\mathbf{n})^2 + (\nabla\times\mathbf{n})^2) \\ f &= \tfrac{1}{2}K(\sin^2\theta\varphi_x^2 + (1-\sin^2\theta\cos^2\varphi)\delta_x^2 + \theta_x^2 \\ &\quad - 2\sin\theta\cos\theta\cos\varphi\varphi_x\delta_x - 2\sin\varphi\delta_x\theta_x). \end{aligned} \tag{7}$$

The index x indicates derivatives towards the x-co-ordinate. With equation (5), expression (7) can be simplified as

$$f_{OF} = \tfrac{1}{2}K\left[(\sin\theta\varphi_x - \cos\theta\cos\varphi\delta_x)^2 + \left(\sin\varphi - \frac{\tan\delta}{\tan\theta}\right)^2\delta_x^2\right].$$

This expression only describes how far the molecules deviate from their parallel positions without containing any information about their positional ordering. However, we could extend this classical energy expression to the case of smectic liquid crystals.

The bending of the layer itself costs energy. In the one-dimensional case, it could be described by a term proportional to the curvature of the layer. One can prove that the mean curvature of a surface K_m equals $-\nabla \cdot \mathbf{k}$, where $\mathbf{k}$ is the unit normal vector on the surface.

$$f_{\text{bend}} = L(\nabla \cdot \mathbf{k})^2 = L\cos^2 \delta \delta_x^2.$$

If we add the cost of the layer thickness variation, for example f_λ°, we get for the total elastic energy

$$f_{\text{elas}}^\circ = T\sin^2(\theta - \theta_0) + L\cos^2 \delta \delta_x^2 + \tfrac{1}{2}K\left[(\sin\theta\varphi_x - \cos\theta\cos\varphi\delta_x)^2 + \left(\sin\varphi - \frac{\tan\delta}{\tan\theta}\right)^2 \delta_x^2\right]. \tag{8}$$

Although this energy expression may seem rather heuristic, it can be useful in drawing conclusions about smectic layer profiles, as is demonstrated in [24].

As a final remark on this energy expression, it should be noted that equation (8) really only contains two independent angles, φ and δ, because of the coupling between δ and θ, see equation (5).

3.1.2.2. *Dahl*

In his introductory study of deformations in the smectic C structure, de Gennes—see [14]—considers small rotations Ω_x, Ω_y and Ω_z in a local reference frame. In [15], expressions of de Gennes are formulated in a fixed laboratory frame. An elasticity theory for compressible smectic layers is given in [16]. There, the elastic energy is composed of five different contributions

$$f_{\text{elas}} = f_s + f_c + f_{cs} + f_* + f_g. \tag{9}$$

The expressions immediately take account of the layer bending energy and the layer thickness variation. In this paper we want to come to a practical form of this energy for some simple one-dimensional simulation studies. With the notation

$$(\nabla_s \mathbf{k})_{ij} = \frac{1}{2}\left[\left(\frac{\partial k_i}{\partial x_j} + \frac{\partial k_j}{\partial x_i}\right)\right],$$

we get the following basic deformations, defined in the same way as in [16]:

$$\left.\begin{aligned}
t_{11} &= -\mathbf{c}\cdot(\nabla_s\mathbf{k})\cdot\mathbf{p} = -\sin\varphi\cos\varphi\cos\delta\delta_x,\\
t_{21} &= -\mathbf{p}\cdot(\nabla_s\mathbf{k})\cdot\mathbf{p} = -\cos^2\varphi\cos\delta\delta_x,\\
t_{31} &= \mathbf{c}\cdot(\nabla\times\mathbf{k}) = \cos\varphi\sin\delta\delta_x,\\
t_{12} &= -\mathbf{c}\cdot(\nabla_s\mathbf{k})\cdot\mathbf{c} = -\sin^2\varphi\cos\delta\delta_x,\\
t_{22} &= -t_{11} = +\sin\varphi\cos\varphi\cos\delta\delta_x,\\
t_{32} &= \mathbf{p}\cdot(\nabla\times\mathbf{k}) = -\sin\varphi\sin\delta\delta_x,\\
t_{13} &= \mathbf{k}\cdot(\nabla\times\mathbf{c}) = -\sin\varphi\cos\delta\varphi_x,\\
t_{23} &= \nabla\cdot\mathbf{c} + \mathbf{p}\cdot(\nabla\times\mathbf{k}) = -\cos\varphi\cos\delta\varphi_x,\\
t_{33} &= -\mathbf{c}\cdot(\nabla\times\mathbf{c}) - \mathbf{c}\cdot(\nabla_s\mathbf{k})\cdot\mathbf{p} = \sin\delta\varphi_x.
\end{aligned}\right\} \tag{10}$$

The different contributions to equation (9) are

$$\left.\begin{aligned} f_s &= \tfrac{1}{2}A_{11}(t_{11})^2 + \tfrac{1}{2}A_{12}(t_{12})^2 + \tfrac{1}{2}A_{21}(t_{21})^2 + \tfrac{1}{2}A_{31}(t_{31})^2 + \tfrac{1}{2}A_{32}(t_{32})^2 \\ &\quad + A_4(t_{11}t_{31}) + A_5(t_{12}t_{32}) + A_6(t_{21}t_{32}) + \bar{B}\gamma^2, \\ f_c &= \tfrac{1}{2}B_1(t_{13})^2 + \tfrac{1}{2}B_2(t_{23})^2 + \tfrac{1}{2}B_3(t_{33})^2 + B_{13}(t_{13}t_{33}), \\ f_{cs} &= C_4(t_{11}t_{13}) + C_2(t_{21}t_{23}) + C_3(t_{31}t_{33}) + C_4(t_{13}t_{31}), \\ f_* &= D_1t_{13} + D_2t_{11} + D_3t_{31} + Dt_{33}, \\ f_g &= E_{v5}(t_{11}^2 - t_{13}t_{31} + t_{12}t_{21} - t_{23}t_{32}) + E_{v6}(-t_{13}t_{31} + t_{11}t_{33}) \\ &\quad + E_{v7}(t_{21}t_{32} + t_{11}t_{13} + t_{11}t_{31} + t_{12}t_{23}) + E_{v9}(-2t_{13}t_{31} - 2t_{23}t_{32}). \end{aligned}\right\} \tag{11}$$

In our coordinate system, these contributions can be calculated with the expressions (10). In § 5, we will give a numerical simulation example. In order to make the calculations easier and to reduce the large number of unknown parameters, we simplify the expressions in the following way. We neglect the so-called gauge terms ($f_g = 0$) and we set

$$A_{11} = 4A, \quad A_{12} = A_{21} = 2A, \quad A_{31} = A_{32} = 0, \quad A_4 = A_6, \quad A_5 = 0, \quad B_1 = B_2 = B_3 = B,$$
$$B_{13} = 0, \quad C_1 = C_2 = C_3 = C, \quad C_4 = 0, \quad \text{and} \quad D_1 = D_2 = D_3 = D.$$

We take f_λ^* (equation (6)) for the layer compression energy. Therefore, we put $\bar{B} = 0$ and replace the corresponding term in equation (11) by expression (6). We get

$$f_{elas}^* = T\left(\frac{\cos\delta - \cos\delta_0}{\cos\delta_0}\right)^2 + A\cos^2\delta\delta_x^2 + B\varphi_x^2 + C\cos\varphi\varphi_x\delta_x + D(\sin\delta - \sin\varphi\cos\delta)(\varphi_x + \cos\varphi\delta_x), \tag{12}$$

(comparable simplifications were made by MacGregor in [18]).

The first term in equation (12) describes the cone angle variation, the second one expresses the deformation of the smectic layers, the third one handles the energy cost of the molecule turning on the smectic cone and the fourth contribution takes the coupling of these two into account. The last term takes care of the chiral energy. Even if we eliminate θ in (8), the coefficients of φ_x^2, δ_x^2 and $\varphi_x\delta_x$ are still different in the expressions (8) and (12). This only indicates that the positional ordering of the molecules has more consequences than accounted for in (8). Full elastic considerations lead to equation (9), as indicated in [15].

3.2. *Electric field energy*

For this important matter, we also refer to [25] and [26]. Depending on the driving conditions of the FLCD, one should consider alternative electric energy expressions. We will mostly consider the one-dimensional case.

3.2.1. **D** *independent of time*

In the case of a time-independent dielectric displacement **D**, which is equivalent to constant surface charge density on the electrodes, we should minimize the Helmholtz

free energy. The electrical part of the volume Helmholtz free energy density is given by

$$f_{\text{elec}}^{\text{H}} = \tfrac{1}{2}\mathbf{E}\cdot\mathbf{D}_{\text{e}} = \tfrac{1}{2}\mathbf{E}\varepsilon_0\bar{\varepsilon}\mathbf{E}, \tag{13}$$

where $\mathbf{D}_{\text{e}}$ is the part of the dielectric displacement that is directly dependent on the electric field (and independent of the polarization density). In one dimension this is

$$D_{\text{ex}} = \varepsilon_0\varepsilon_{xx}E_x.$$

Using

$$D_x = \varepsilon_0\varepsilon_{xx}E_x + P_x = \varepsilon_0\varepsilon_{xx}E_x - P\cos\varphi\cos\delta,$$

we can write

$$f_{\text{elec}}^{\text{H}} = \frac{1}{2\varepsilon_0\varepsilon_{xx}}(D_x + P\cos\varphi\cos\delta)^2. \tag{14}$$

For exact analysis, equation (2) should be used for ε_{xx}. This complicates formula (14) rather drastically. As we will see in § 4, a variable ε_{xx} makes our numerical method practically impossible. As a first order approximation, we take $\varepsilon_{xx} = (\varepsilon_{\parallel} + \varepsilon_{\perp})/2$. This means that for ferroelectric liquid crystal simulations, the anisotropy of the dielectric tensor will be neglected in the first instance compared with the major electrical effect—the orientation of the polarization.

3.2.2. *ΔV independent of time*

If ΔV, the voltage drop over the display, is kept constant, the formulae look even more complicated. In this case, we should consider the so-called Gibbs free energy

$$f_{\text{elec}}^{\text{G}} = -\tfrac{1}{2}\mathbf{E}\cdot\mathbf{D}_{\text{e}} - \mathbf{E}\cdot\mathbf{P} = -\tfrac{1}{2}\mathbf{E}\varepsilon_0\bar{\varepsilon}\mathbf{E} - \mathbf{E}\cdot\mathbf{P}. \tag{15}$$

Flexoelectric effects—see [16]—are not included. From here we treat equation (15) in one dimension

$$f_{\text{elec}}^{\text{G}} = -\tfrac{1}{2}\varepsilon_0\varepsilon_{xx}E_x^2 - E_xP_x. \tag{16}$$

The complication is that neither E_x nor D is constant. In order to express equation (16) in terms of the basic variables (the angles φ and δ), we have to eliminate E_x. We start with Gauss' law (in one dimension) without charge accumulation in the bulk

$$\frac{\partial}{\partial x}(D_x) = 0$$

or

$$\frac{\partial}{\partial x}(\varepsilon_{xx}E_x) = -\frac{1}{\varepsilon_0}\frac{\partial}{\partial x}P_x.$$

Therefore

$$\varepsilon_{xx}E_x = -\frac{P_x}{\varepsilon_0} + C.$$

The integration constant C can be determined with the condition

$$\int_0^d E_x = -\Delta V.$$

The calculations are straightforward. We get for the electric field

$$E_x = -\frac{\Delta V}{\varepsilon_{xx}\int_0^d \frac{dx}{\varepsilon_{xx}}} + \frac{P}{\varepsilon_0\varepsilon_{xx}}\cos\varphi\cos\delta - \frac{P\int_0^d \frac{\cos\varphi\cos\delta}{\varepsilon_{xx}}dx}{\varepsilon_0\varepsilon_{xx}\int_0^d \frac{dx}{\varepsilon_{xx}}}. \tag{17}$$

This looks prettier, when the x-dependence of ε_{xx} is neglected

$$E_x = -\frac{\Delta V}{d} + \frac{P}{\varepsilon_0\varepsilon_{xx}}\cos\varphi\cos\delta - \frac{P}{\varepsilon_0\varepsilon_{xx}d}\int_0^d \cos\varphi\cos\delta dx. \tag{18}$$

Nevertheless, when substituted in equation (15), both (17) and (18) result in a complex formula. Indeed, simulations simplify when the dielectric displacement D is taken as parameter. Therefore in this context, we prefer the Helmholtz expressions (13) and (14) to the corresponding Gibbs expressions (15) and (16). For a fixed D-value, the corresponding voltage drop across the liquid crystal layer is obtained afterwards from the equilibrium angle distribution.

3.3. *Surface energy*

In this article, we consider a simple classical surface energy contribution. With **s** the outward normal to the glass plates, **n** the director and **p** the unit vector in the direction of the macroscopic polarization, we can write

$$f_{\text{surf}} = \gamma_1(\mathbf{n}\cdot\mathbf{s})^2 - \gamma_2(\mathbf{p}\cdot\mathbf{s}). \tag{19}$$

The first term tends to put the molecule near the glass surface as horizontal as possible; the second term pulls the polarization vector as perpendicular to the surface as possible. If we want to simulate very 'hard' boundary conditions (for example, the molecule at the border is not allowed to deviate from the horizontal position), we can take very large values for γ_1 and γ_2.

The chevron profiles that we will model will be symmetric. The function $\delta(x)$ will be antisymmetric, the top of the chevron always being in the mid-plane of the LC-cell. This is a way to meet the so-called no-slip condition for the smectic layers, which states that the layer is anchored at the bottom and the top glass.

4. Direct minimization

Equations (12), (14) and (19) are the starting point for a minimization program. Wöhler *et al.*—for example, see [26]—have already discussed a similar calculation technique for the case of nematic liquid crystals. It has been implemented for nematic LCDs by several authors—for example, [27].

Instead of deriving the Euler–Lagrange equations, we directly minimize the energy expression (4). The method with time-independent dielectric displacement has been chosen—see § 3.2.1. For this method the electric energy is less complicated.

We look for the functions $\delta(x)$ and $\varphi(x)$ that *minimize* the following functional

$$\begin{aligned}\mathscr{F} = \int_0^d \Big[& A(\cos\delta)^2\delta_x^2 + B\varphi_x^2 + C\cos\varphi\varphi_x\delta_x \\ & + D(\sin\delta - \sin\varphi\cos\delta)(\varphi_x + \cos\varphi\delta_x) + T(\cos\delta - \cos\delta_0)^2 \\ & + \frac{1}{2\varepsilon_0\varepsilon_{xx}}(D + P\cos\varphi\cos\delta)^2\Big]dx + \gamma_1(n_{1t}^2 + n_{1b}^2) + \gamma_2(-p_{1t} + p_{1b}),\end{aligned} \tag{20}$$

with

$$\left.\begin{aligned} n_1 &= -\sin\theta\sin\varphi\cos\delta + \cos\theta\sin\delta \\ \text{and} \\ p_1 &= -\cos\varphi\cos\delta \end{aligned}\right\} \tag{21}$$

where t and b indicate the top and bottom values at $x = d$ and $x = 0$, respectively. φ_x and δ_x are the derivatives of the angles with respect to x. The function $\delta(x)$ will be antisymmetric with respect to the midplane. There are no restrictions for $\varphi(x)$. We shall transform the integral (20) into a multidimensional function. First we consider the normalization

$$\xi = \frac{x}{d},$$

$$\varphi_x = \frac{\partial\varphi}{\partial x} = \frac{\partial\varphi}{\partial\xi}\cdot\frac{1}{d}.$$

The layer thickness ($0 < \xi < 1$) is divided into a number of intervals, in which the unknown functions $\varphi(x)$ and $\delta(x)$ are approximated by linear functions. For instance, between the interval points ξ_i and ξ_{i+1}, the function $\varphi(\xi)$ is replaced by the linear function $\varphi^*(\xi)$

$$\varphi^*(\xi) = \varphi_i + \frac{\Delta\varphi}{\Delta\xi}(\xi - \xi_i).$$

We use the symbol $\Delta\varphi = \varphi_{i+1} - \varphi_i$.

The integral (20) can be split into a sum of subintegrals with respect to the intervals $[\xi_i, \xi_i + 1]$. As an example, we consider the electric part E_i. First we introduce some new symbols.

$$\left.\begin{aligned} \chi &= 2\varphi, \\ \psi &= 2\delta, \\ \delta f(\varphi,\delta) &= f(\varphi_{i+1},\delta_{i+1}) - f(\varphi_i,\delta_i), \\ E_i &= \int_{\xi_i}^{\xi_{i+1}} \frac{d}{2}\varepsilon_0\varepsilon_{xx}E^2\,d\xi \\ &= \frac{d}{2\varepsilon_0\varepsilon_{xx}}\int_{\xi_i}^{\xi_{i+1}} (D_x + P\cos\varphi\cos\delta)^2\,d\xi \\ &= \frac{d\Delta\xi}{2\varepsilon_0\varepsilon_{xx}}\left\{D_x^2 + 2PD_x\frac{\Delta\varphi\Delta\sin\varphi\cos\delta - \Delta\delta\Delta\cos\varphi\sin\delta}{(\Delta\varphi)^2 - (\Delta\delta)^2}\right. \\ &\quad \left. + \frac{P^2}{4}\left[1 + \frac{\Delta\sin\chi}{\Delta\chi} + \frac{\Delta\sin\psi}{\Delta\psi} + \frac{\Delta\chi\Delta\sin\chi\cos\psi - \Delta\psi\Delta\cos\chi\sin\psi}{(\Delta\chi)^2 - (\Delta\psi)^2}\right]\right\} \end{aligned}\right\} \tag{22}$$

One can see that the integration leads to rather complicated formulae. Also this integration is only possible if a constant ε_{xx} is used. If one would use equation (3) instead, the integration becomes far more complicated. (One must even eliminate θ first with equation (5).)

With the technique as demonstrated in the formulae (22), the Helmholtz free energy becomes a function of the values φ_i and δ_i at the interval boundaries. This multi-

dimensional function is minimized. The technique is called the modified Ritz method for the calculation of variational problems—see [28]. The minimization of the function itself is done by a modified Newton–Raphson method with second order of convergence. Special care is necessary to avoid inappropriate extrema, such as maxima and saddle points. For the details of the simulation program, we wish to refer to [29]. A lot of analytical calculations are necessary. Not only the integrals themselves, but the first and second derivatives with respect to the node values ($\varphi_i \ldots$) must be calculated. Moreover, in order to avoid numerical problems, one should expand the formulae as (22) in a Taylor series, where the denominator disappears.

5. Simulation results

In order to illustrate the use of our energy expressions, as well as the possibilities of the simulation technique, we give the following example. The $\varphi(x)$ and $\delta(x)$ distributions are calculated for a typical FLCD-structure, thickness 2 μm. The numerical values for the different parameters are given in the table. For the relative magnitudes of the elastic constants, we made the following considerations. T/A is chosen in such a way that the chevron profile bends only slightly when a voltage is applied—see also [10] and [24]. The other constants were chosen is comparison with the classical

The numerical values for the parameters utilized.

Parameter	Value	Parameter	Value
A	1·0 pN	P	$-300\ \mu C\ m^{-2}$
B	0·5 pN		
C	− 0·9 pN	$\varepsilon_{parallel}$	5·0
D	$0{\cdot}5\ \mu N\ m^{-1}$	ε_{perp}	5·5
T	500 000 pa		
θ_0	22·5°	γ_1	$30\ \mu N\ m^{-1}$
ν	0·96	γ_2	$-30/0/+30\ \mu N\ m^{-1}$

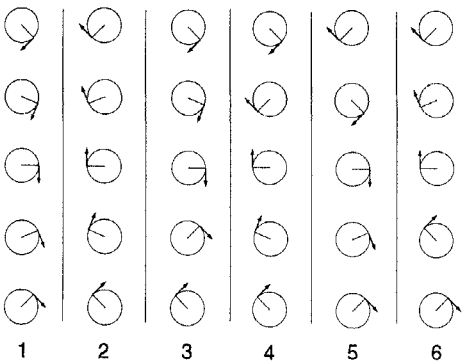

Figure 3. The position of the molecules on the smectic cone in each of the six configurations. The arrows represent the polarization vectors. The position of the molecules at the bottom and top glass plate (respectively bottom and top circle) is horizontal. State 1 is uniform, down; 2 is uniform, up; 3 splayed down, inward; 4 splayed up, inward; 5 splayed down, outward; 6 splayed up, outward. For our parameter set (with a negative macroscopic polarization), states 1, 3, and 5 occur when the electric field is downward and 2,4 and 6 for an upward electric field.

Oseen–Frank expression f_{elas}° in equation (8). Furthermore, the stability relationships from Dahl and Lagerwall [15] had to be fulfilled. With the current simplifications, this means that $A > 0$, $B > 0$, $2AB - C^2 > 0$.

Depending on the specific choice of the polar coupling ($\gamma_2 = -30$, 0 or $+30\,\mu N\,m^{-1}$) at the alignment layers and the orientation of the electric field, we can make distinctions amongst six different configurations. In figure 3 these cases are illustrated by the position of the molecules on the smectic cone through the slab. The arrows illustrate the orientation of the polarization vector $P\mathbf{p}$, the case $P < 0$. Therefore the direction of the arrows is opposite to the direction of $\mathbf{p}$ in equation (19). Both glass plates are considered to have the same coupling characteristics. In general one might expect the following molecular distributions, depending on the signs of γ_2 and $E \cdot P$:

	$EP > 0$	$EP < 0$
$\lvert\gamma_2\rvert \approx 0$	1	2
$\gamma_2 > 0$	3	4
$\gamma_2 < 0$	5	6

We can use the following names for these six distributions

$P > 0$	$P < 0$
1. Uniform up	Uniform down
2. Uniform down	Uniform up
3. Splayed up, outward	Splayed down, inward
4. Splayed down, outward	Splayed up, inward
5. Splayed up, inward	Splayed down, outward
6. Splayed down, inward	Splayed up, outward

For the uniform state and the outward and inward splayed states, there are always two alternatives: an upward and downward configuration. This illustrates the bistability

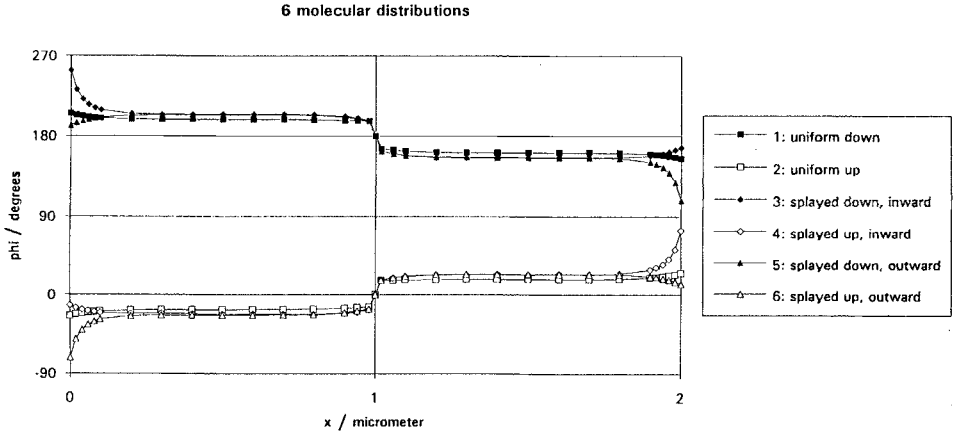

Figure 4. The $\varphi(x)$ distribution under an applied voltage for each of the six configurations, when the applied voltage is minimal (the results of the simulations were -4 mV, 8 mV, -13 mV, 11 mV, -7 mV and 11 mV for the six states, respectively).

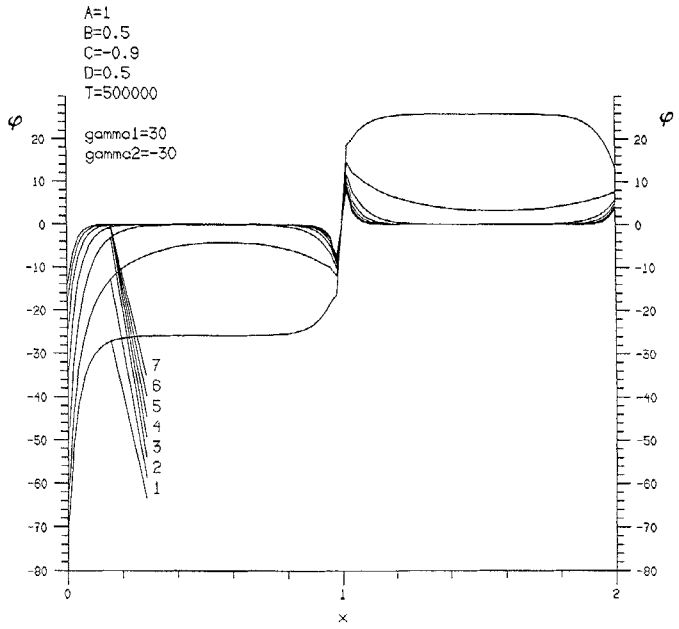

Figure 5. φ-distributions for different voltages in state 6: for 1 to 7, respectively, 0·021 V, 0·247 V, 1·84 V, 3·95 V, 6·08 V, 8·22 V and 10·37 V.

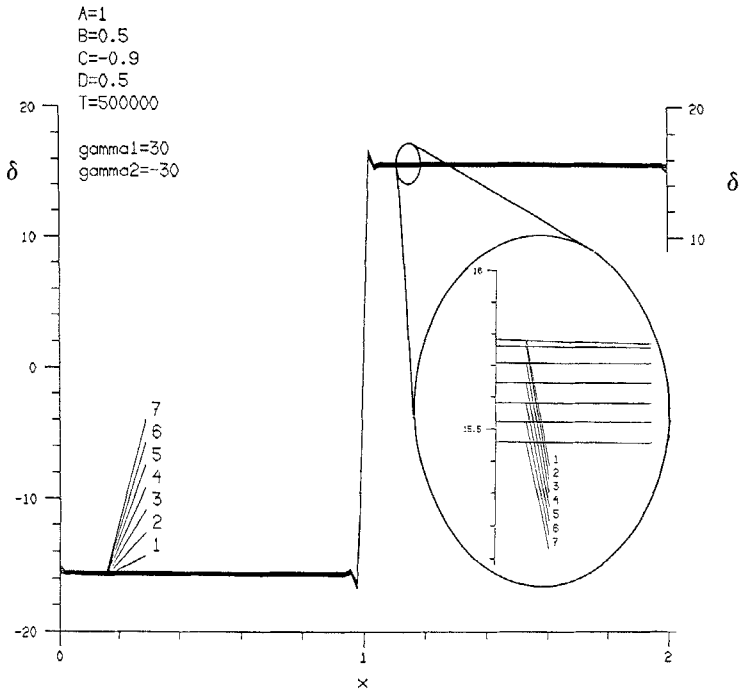

Figure 6. δ-distributions for different voltages in state 6.

of the device. Figure 4 shows the six simulated $\varphi(x)$-functions, for small voltage drops.

The magnitude of the γ-values corresponds with [30]. Remember that with this simulation technique, we cannot require the voltage drop to be exactly equal to zero. Trial and error, with several values for D, leads to the depicted curves for very small voltages (in absolute value less than 15 mV). In the present simulation P is negative, and therefore the splayed state 6, for example, occurs when positive voltages are applied. Figures 5 and 6 show how the molecular distribution for this state 6 changes with the applied voltage. It is noted that a small voltage already suffices to pull the molecules towards the ($\varphi = 0$)-state, where the polarization vector is as vertical as possible. Because of the high value for the parameter T, δ does not change substantially with increasing voltage.

6. Conclusions

With a fixed reference frame, we have calculated the different contributions to the free energy that is minimized in FLCD-structures. The layer structure has been included in the equations. Complicated general expressions can be simplified in the one-dimensional case. The number of parameters is reduced. One of the possible energy expressions has been used in a strong minimization program, that produces valuable simulations. Constant electrode charge calculations are easier to fulfil. More experimental data for the different parameters could lead to a deeper insight into the chevron structure of FLC-cells.

This work was supported by the Belgium Fund for Scientific Research (NFWO).

References

[1] CLARK, N. A., and LAGERWALL, S. T., 1980, *Appl. Phys. Lett.*, **36,** 899.
[2] CLARK, N. A., and LAGERWALL, S. T., 1986, *Jap. Display '86*, SID, 456.
[3] NAKAGAWA, M., ISHIKAWA, M., and AKAHANE, T., 1988, *Jap. J. appl. Phys.*, **27,** 456.
[4] OUCHI, Y., TAKEZOE, H., and FUKUDA, A., 1987, *Jap. J. appl. Phys.*, **26,** L21.
[5] CLARK, N. A., RIEKER, T., and MACLENNAN, J., 1988, *Ferroelectrics*, **85,** 79 (presented at the 1st FLC Conference, 1987, Arcachon).
[6] CLARK, N. A., and RIEKER, T., 1988, *Phys. Rev.* A, *Rap. Commun.*, **37,** 1053.
[7] RIEKER, T., CLARK, N. A., SMITH, G., PARMAR, D., SIROTA, E., and SAFINYA, C., 1987, *Phys. Rev. Lett.*, **59,** 2658.
[8] HARTMANN, W., VERTOGEN, G., GERRITSMA, C., VAN SPRANG, H., and VERHULST, A., 1989, *Europhysics Lett.*, 657.
[9] HARTMANN, W., VERTOGEN, G., GERRITSMA, C., VAN SPRANG, H., and VERHULST, A., 1991, *Ferroelectrics*, **113,** 257. Presented at the 2nd FLC Conference, 1989, Göteborg.
[10] WILLIS, P. C., CLARK, N. A., and SAFINYA, C. R., 1992, *Liq. Crystals*, **11,** 581.
[11] WILLIS, P., THOMAS, B., HARTMANN, W., CLARK, N. A., and SAFINYA, C. R., 1992, *14th International Liquid Crystal Conference*, Pisa, Poster presentation C-P68.
[12] WILLIS, P., HARTMANN, W., THOMAS, B., CLARK, N. A., and SAFINYA, C. R., 1992, *14th International Liquid Crystal Conference*, Pisa, Poster presentation C-P70.
[13] YANG, F., and SAMBLES, J. R., 1993, *Liq. Crystals*, **13,** 1.
[14] DE GENNES, P. G., 1974, *The Physics of Liquid Crystals* (Clarendon Press), pp. 314–323.
[15] DAHL, I., and LAGERWALL, S. T., 1984, *Ferroelectrics*, **58,** 215.
[16] DAHL, I., 1991, *Ferroelectrics*, **113,** 121.
[17] NAKAGAWA, M., 1990, *Liq. Crystals*, **8,** 651.
[18] MACGREGOR, A. R., 1989, *J. Am. opt. Soc.* A, **6,** 1493.
[19] LESLIE, F., 1992, *14th International Liquid Crystal Conference, Pisa*, Oral presentation.
[20] JONES, J. C., TOWLER, M., and RAYNES, E. P., 1991, *Ferroelectrics*, **121,** 91. Presented at the 3rd FLC Conference, 1991, Boulder.

[21] JONES, J. C., and RAYNES, E. P., 1992, *Liq. Crystals*, **11,** 199.
[22] NAKAGAWA, M., 1990, *J. phys. Soc., Japan*, **55,** 1995.
[23] LIMAT, L., and PROST, J., 1993, *Liq. Crystals*, **13,** 101.
[24] DE MEYERE, A., PAUWELS, H., and DE LEY, E., 1993, *Liq. Crystals*, **14,** 1269.
[25] PAUWELS, H., and CUYPERS, F., *Ferroelectrics*, **113,** 37. Presented at the 2nd FLC Conference, 1989, Göteborg.
[26] WÖHLER, H., FRITSCH, M., HAAS, G., and MLYNSKI, D., 1989, *Jap. Display '89*, SID, 376.
[27] CUYPERS, F., 1989, Ph.D. thesis, Rijksuniversiteit Gent.
[28] STRANG, G., 1986, *Introduction to Applied Mathematics* (Wellesley Cambridge Press).
[29] DE MEYERE, A., 1994, *Comput. Phys. Commun.*, **79,** 353.
[30] DE LEY, E., and PAUWELS, H., 1990, *Eurodisplay '90*, SID, 264.